Received 00th January 20xx,
Accepted 00th January 20xx

DOI: 10.1039/x0xx00000x

www.rsc.org/

A protein nanocontainer targeting epithelial cancers: rational engineering, biochemical characterization, drug loading and cell delivery

Caroline Ladurantie[a]†, Mathilde Coustets[a,b]†, Pascal Demange[a], Serge Mazeres[a], Stéphanie Dauvillier[a], Georges Czaplicki[a], Justin Teissié[a], Marie-Pierre Rols[a], Alain Milon[a], Vincent Ecochard[a], Grégori Gross[a,c] and Laurent Paquereau[a]*

[a] *Institut de Pharmacologie et Biologie Structurale, IPBS, Université de Toulouse, CNRS, UPS, 205 Route de Narbonne, BP64182, 31077 Toulouse, France. E-mail : Laurent.Paquereau@ipbs.fr*
[b] *Present address: Urosphere, Parc technologique du canal, Canal Biotech II, 3 rue des satellites 31400 Toulouse, France.*
[c] *Present address: GTP Technology, Bâtiment Gould – 52 l'Occitane, 31670 Labège Cedex-France.*
† These authors contributed equally to the work.
Electronic Supplementary Information (ESI) available: [details of any supplementary information available should be included here]. See DOI: 10.1039/x0xx00000x

Journal Name

ARTICLE

Electronic Supplementary Information

Tetrameric behavior in solution: Analytical Ultracentrifugation and Dynamic Light Scattering

Ultracentrifugation data showed that XCL displays a sedimentation coefficient of 4.53 Svedberg that fits a molecular weight of 58 kDa (Fig S1A), close to the 64 kDa weight of the homotetrameric assembly of XCL. Diffusion light scattering experiments confirmed this result. Indeed, we obtained a single peak displaying a hydrodynamic radius of 3 nm corresponding to a homotetrameric structure (Fig S1B).

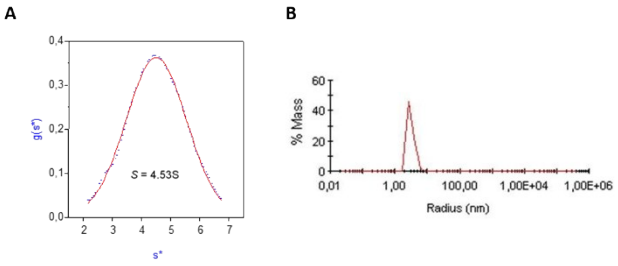

Figure S1: A) Velocity sedimentation studies were carried out à 20 °C with a Beckman model XL-A ultracentrifuge equipped with a four-hole AN-55 rotor and standard 1.2cm double sector cells. The native XCL protein at 25µM in 25mM sodium phosphate buffer pH7 was loaded into the protein compartment of the double-sector cell and the solvent compartment was loaded with the protein buffer. Centrifugation was realized at 40,000rpm and 200 radial scans of absorbance at 280nm were taken every minutes. The Sednterp program was used to calculated solvent density (1.0018g/cm) and partial specific volume (0.7268ml/g) from amino acid composition. The sedimentation data were analysed with the program Sedfit.35 Continuous C(s) and c(M) distributions were examined. B) DLS: samples of 150µM (filtered on disposable 0.1µm filters) were analysed at 20.5°C using DynaPro Nanostar instrument (Wyatt Technology). The data were analysed with Dynamics software (Wyatt Technology)

Overall topology of the native and mutated protein

The sequences of the XCL protein and the double mutant T12C/A38C were aligned using the structural data. The secondary structures are mainly composed of beta strands and explain the very high stability of the protein. The T12C and A38C mutations are localized in the regions involved in the formation of the tetramer and outside or at the end of the beta 1 and beta 3 strands.

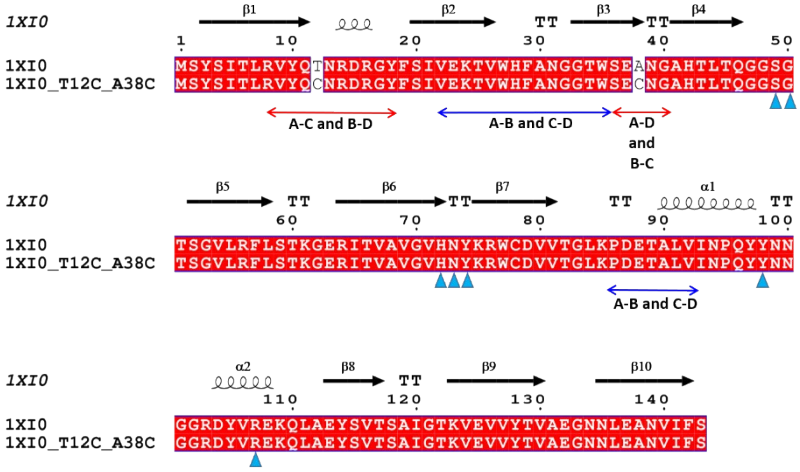

Figure S2: Primary sequence and secondary structures of XCL (1XI0) and the mutant T12C-A38C (1XI0_T12C_A38C). The interfaces of the dimeric assemblies are underline in blue. The interfaces leading to the tetrameric nanocontainer are underline in red. The residues involved in T antigen binding site are indicated (blue triangle). Figure was realized with EndScript[1].

Therefore, these positions do not have a negative impact on the overall stability of the protein. In addition, these two mutations do not interfere with the residues involved in the formation of the T antigen binding site.
(GenBank accession number: AF338359; RCSB Protein Data Bank access code: 1XI0).

Oxidation and reduction conditions

The oxidation of the A38C mutant was tested by DSF in the absence or presence of an oxidizing agent (GSSG-data not shown). The results showed spontaneous and rapid oxidation of the disulfide bridges for this mutant (Fig S3A). Alkylation of cysteines with iodoacetamide after reduction was also analyzed. It was interesting to note that the loops that closed the access to the inner cavity also contributed to the overall stability of the protein since the alkylated protein was less stable than the reduced form.
The reduction of disulfide bridges in A38C mutant was tested with different reducing agents (DTT, TCEP, βME). The effectiveness of the reduction was measured by DSF (Fig S3B). Only DTT allowed to reduced efficiently disulfides bonds of the A38C mutant.

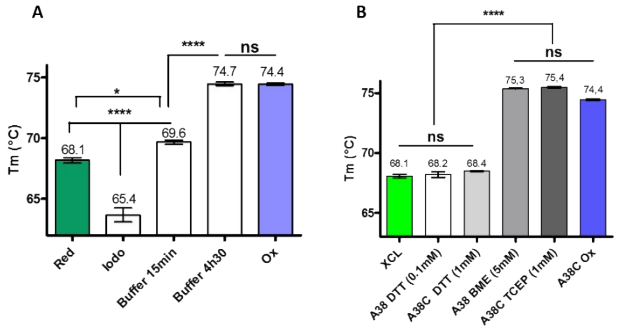

Figure S3: DSF experiments A) Oxidization of reduced A38C in phosphate buffer was analysed at the indicated times. Alkylation of reduced cysteines was also analysed after incubation with iodoacetamide. B) Different reducing compounds were analysed to test their effectiveness on the A38C mutant. DTT: Dithiotreitol; BME: β-mercaptoethanol; TCEP: tris(2-carboxyethyl)phosphine. n≥5 independent experiments.

Raw data of apparent Kdiss measurement: Size Exclusion chromatography, FRET and Isothermal Titration Microcalorimetry experiments

The reversible dissociation equilibrium of XCL highlighted by FRET between tetramer and dimer should be shifted to dissociation after dilution and thus allowing the measurement of an apparent global dissociation constant. Equilibrium displacement was assessed by gel filtration chromatography (SEC). At high concentration (10µM), XCL displayed an elution volume of 13.2mL close to the elution volume of BSA as expected for a tetrameric species (Fig S4A). We performed several injections using varying concentrations of XCL and observed the elution of the protein as a single peak. This peak was shifted toward longer elution volumes as the concentration was lowered, indicating a smaller molecular weight. The figure S3B showed the profile obtained in FRET with different concentrations of the FITC-XCL/RITC-XCL mix. Isothermal titration calorimetry (ITC) was used to determine thermodynamic parameters of the tetramer assembly. In this method, a concentrated solution of XCL was diluted into buffer, and the heat of dissociation to dimers was measured (Fig S4C).

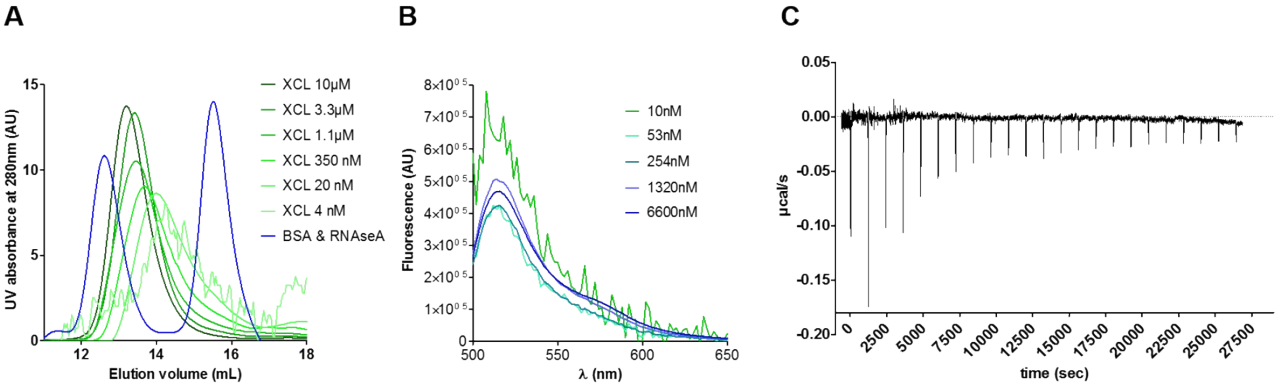

Figure S4: A) SEC was carried out with a concentration range between 10µM and 4nM of XCL. UV absorbance (280nm) was measured in function of elution volume B) The FITC-XCL/RITC-XCL mix was diluted at different concentrations and incubated 1 hour at room temperature in order to reach steady state. Fluorescence spectra were recorded with a 468 nm excitation light. To visualize all the curves, each fluorescence intensity was corrected by the dilution factor. C) A concentrated solution of XCL (40µM) was diluted into buffer, and the heat of dissociation to dimers was measured by ITC.

Acidic behaviour of XCL and A38C: Size Exclusion chromatography

We were able to demonstrate the formation of dimers and monomers by SEC carried out at two pH. At pH 7, XCL was eluted in tetrameric form and it was only at pH 4.4 that a dimeric form was detected. Only one experimental condition tested allowed us to highlight the monomeric forms of XCL by the addition of a very low concentration of SDS at pH 4.4 (Fig S5). In a way, it seems that SDS played the role of "lever" to separate dimers in monomers. The same “lever” effect was observed for A38C oxidized which highlighted the dimer formation (Fig S5). As the experience was not carried out under reducing conditions, obviously for this mutant the monomer cannot be generated.

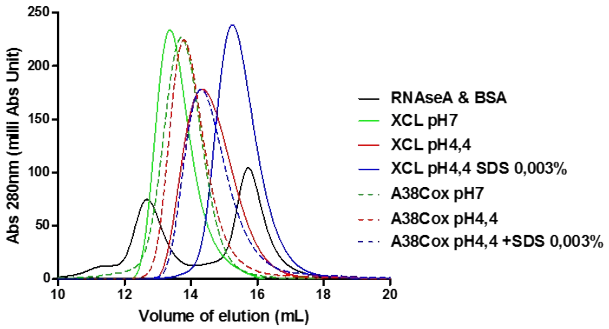

Figure S5: SEC was performed at different pH values with XCL and the A38C oxidized mutant. The monomer was only detected in the presence of 0.003% SDS. BSA (66KDa) and RNAse A (13.7KDa) were used as references.

Redox potential of Doxorubicin

The redox potential of doxorubicin (-320mV[2]) is in the same range to the one of DTT (-330mV). In presence of DTT as reducing agent, 53% of the nanocontainer was loaded and when the incubation was realized without DTT, a 45% loading rate was reached.

Therefore, doxorubicin was able to reduce itself the disulfide bridges of the A38C nanocontainer but DTT improved the loading rate.

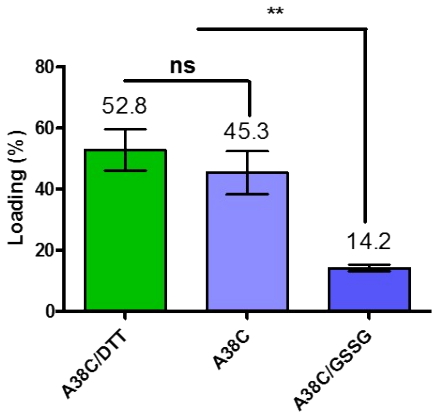

Figure S6: Doxorubicin was incubated for 24h with A38C in presence of DTT (A38C/DTT), with A38C alone (A38C) or in presence of GSSG (A38C/GSSG). n≥5 independent experiments.

Analysis of cell cycle by FACS

Cell cycle phases were analyzed by FACS after labelling of cells with propidium iodide. We checked the impact of high amount of empty nanocontainer on cell behavior by incubating OVCAR-3 cells with 5.5µM (350µg/ml) of empty nanocontainer and the results showed that the nanocontainer did not significantly modify the cell cycle (Fig S7B). Cells were incubated with the A38C-Doxo nanocontainer at 1.6µM (100µg/ml) (Fig S7C) and 5.5µM (350µg/ml) (Fig S7D). In these condition cells were mainly blocked in G2/M phase which was characteristic of the doxorubicin effect (compared to the doxorubicin effect alone Fig S7E).

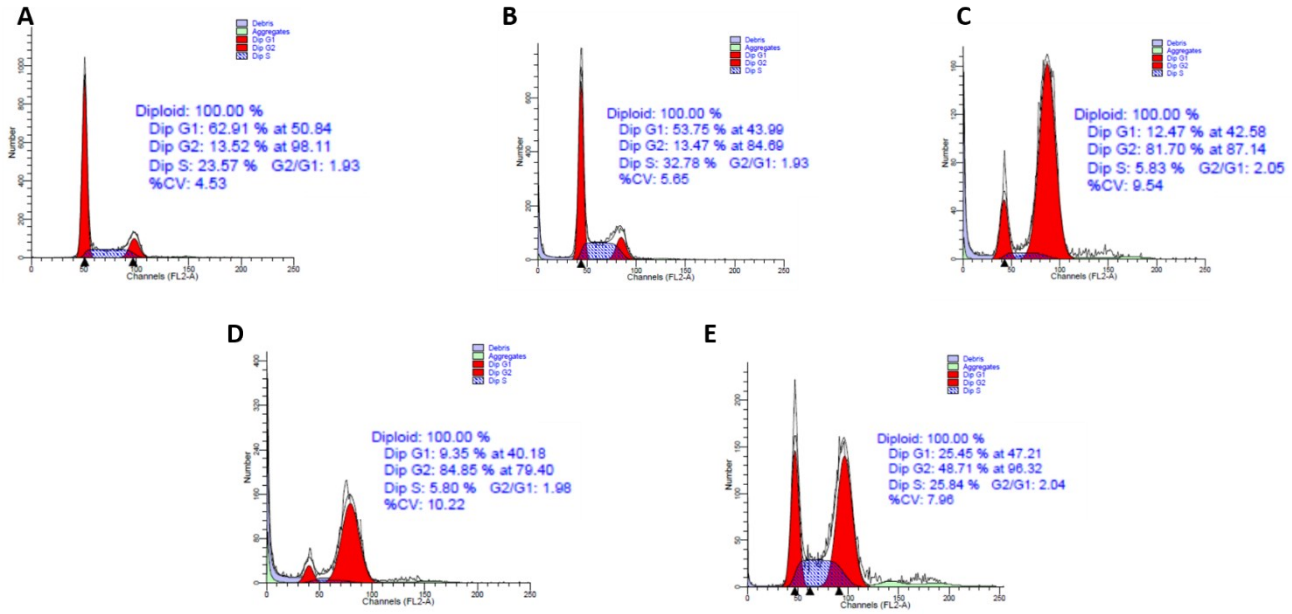

Figure S7: FACS profiles obtained for OVCAR3 cell A) untreated B) incubated with the empty A38C nanocontainer (5.5µM - 350µg/ml) C) A38C-Doxorubicine (1.6µM - 100µg/ml) D) A38C-Doxorubicine (5.5µM - 350µg/ml) E) 1µM of doxorubicine incubated for 30 min with OVCAR-3 cells before PBS washing. Cells were then cultured 48h more before analysis of cell cycle.

1. X. Robert and P. Gouet, *Nucleic acids research*, 2014, 42, W320-W324.
2. S. Vandenwijngaert, M. Swinnen, A. S. Walravens, M. Beerens, H. Gillijns, E. Caluwe, R. E. Tainsh, D. I. Nathan, K. Allen, P. Brouckaert, J. Bartunek, M. Scherrer-Crosbie, K. D. Bloch, D. B. Bloch, S. P. Janssens and E. S. Buys, *Antioxidants & redox signaling*, 2017, 26, 153-164.